International Journal of Refrigeration 138 (2022) 148–158

Contents lists available at ScienceDirect

International Journal of Refrigeration

journal homepage: www.elsevier.com/locate/ijrefrig

Techno-economic control strategy optimization for water-source heat pump coupled with ice storage district cooling system

Optimisation de la stratégie de régulation technico-économique pour une pompe à chaleur à eau couplée à un systéme de refroidissement urbain avec stockage de glace

Qiong Chen [a,b], Wenhan Wei [a,b,c], Nan Li [a,b,*]

[a] National Center for International Research of Low-Carbon and Green Buildings, Ministry of Science and Technology, Chongqing University, Chongqing 400044, China
[b] Department of Civil Engineering, Chongqing University, Chongqing 400044, China
[c] Central-South Architectural Design Institute, Wuhan, 430071, China

ARTICLE INFO

Keywords:
Renewable energy
Ice storage
District cooling system
Control strategy optimization
Genetic algorithm

Mots clés:
Énergie renouvelable
Stockage de glace
Systéme de refroidissement urbain
Optimisation de la stratégie de régulation
Algorithme génétique

ABSTRACT

Incorporating low-temperature renewable energy sources such as geothermal energy, solar energy, and waste heat into district heating and cooling systems is expected to be an effective solution for reducing fossil energy consumption and carbon emissions. This study aims to propose an optimal intelligent control strategy for the water-source heat pump coupled with an ice storage district cooling system, which can fully maximize the economic potential of renewable energy and ice storage systems. The proposed control strategy treats the ice melt cooling rate, water supply temperature, and cooling ratio of the water source heat pump as three independent control variables. The minimum operating cost per unit of cooling supply is identified as the optimal objective function of the genetic algorithm. An integrated heat transfer model of the water-source heat pump coupled with an ice storage district cooling system was developed, and experimental test data verified its accuracy. Compared with the ice melting priority control strategy and the water-source heat pump priority control strategy, the GA-based optimal control strategy saved 8.7–9.3% of the operating cost while maintaining a relatively good energy-saving performance. This proposed intelligent control strategy can stimulate the tremendous economic potential of the ice storage district cooling system coupled with renewable energy sources.

1. Introduction

Building energy consumption, one of the three main components of energy consumption, accounts for 36% of the world's total energy consumption (Xu et al., 2020) while the energy consumption share of heating ventilation and air conditioning (HVAC) systems serves as the most prominent section accounting for about 60–70% of the total energy consumption of buildings (Allen et al., 2020; Wang et al., 2021a). In the actual operation, there is a common problem of low average load rate, high peak load rate, and low efficiency of power utilization (Sun et al., 2020) which will quickly lead to the insufficient power supply of the power grid during peak load hours and excess power during valley load hours (Wang et al., 2021b).

To address the above problems and ensure the smooth operation of the power system, the previous research and relative policies on scientific management of the power-demand side are gradually increasing and being implemented (Alajmi and Zedan, 2020; Inayat and Raza, 2019; Han et al., 2021). Large-scale district heating and cooling systems (DHCS) (Deng et al., 2017), as a centralized set-up of large energy stations and one of the energy-saving solutions for HVAC systems, are increasingly being integrated with renewable sources and ice storage technology (Anderson et al., 2021) which has become an effective solution for carbon dioxide emission reduction and energy efficiency improvement (Abugabbara et al., 2020).

There is plenty of state-of-the-art research on district heating and cooling systems focusing on system design optimization (Falay et al., 2020; Coccia et al., 2021) Chan et al. (2007). developed the optimal design approach for the distribution pipe configurations of district

* Corresponding author at: National Centre for International Research of Low-Carbon and Green Buildings, Ministry of Science and Technology, Chongqing University, Chongqing 400044, China.
E-mail address: nanlicqu@163.com (N. Li).

https://doi.org/10.1016/j.ijrefrig.2022.03.010
Received 11 December 2021; Received in revised form 20 January 2022; Accepted 5 March 2022
Available online 7 March 2022

cooling.

Nomenclature

T_{eo}	The chilled water supply temperature on the evaporation side, °C.	γ	The ice melting cooling ratio (the percentage of cooling supply of ice storage system.
T_{ei}	The chilled water return temperature on the evaporation side, °C.	θ	The cooling supply proportion of the WSHP unit to the total cooling supply.
T_{ci}	The cooling water inlet temperature on the condensation side, °C.	g	The ethylene glycol solution.
T_{co}	The cooling water outlet temperature on the condensation side, °C.	b	The evaporation pump of WSHP.
T_{gei}	The supply temperature of the ethylene glycol solution, °C.	BS	The evaporation pump of DMHP.
T_{geo}	The return temperatures of the ethylene glycol solution, °C.	BQ	The river water pump.
q	The cooling supply at a specific moment, kW.	B	The condensation pump of WSHP.
Q	The cooling supply, kW.	BY	The ethylene glycol pumps.
W	The power consumption, kW.	B1	The primary chilled water pump.
COP	The coefficient of performance.	Br	The chilled water pump for ice melting.
m	The flow rate of the refrigerant, m^3 /h.	B2	The circulation water pump for the external network system.
M	The flow rate of the refrigerant, kg /h.	WSHP	Water-source heat pump
C	The specific heat capacity of the refrigerant, J /kg· °C.	DMHP	Dual-model water-source heat pump.
H	The pump head, m.	DMHP, COOL	Cooling model of DMHP.
η	The pump efficiency.	DMHP, IS	Ice storage mode of DMHP.
β	The ratio of melted ice to the total ice storage volume.	DCS	District cooling system.
ε	The ice melting rate.	PTHE	Plate-type heat exchangers.
δ	The discharge capacity.	PTHE (IM)	Plate-type heat exchangers for ice melting.

systems (DCS) by applying a genetic algorithm (GA) combined with local search techniques Chiam et al. (2019). proposed a hierarchical design optimization framework for DCS to solve complex mixed integer nonlinear programming problems in their research Kang et al. (2019). proposed a new optimal design method for the DCSs to improve cost-effectiveness and energy efficiency. The developed approach was tested in a practical case study at a university campus in Hong Kong. The results showed that the optimal design method helped save 9.6% of primary energy and significantly reduced operating costs by 44%. Besides, a lot of control method research has been conducted for the energy-saving improvements of DHCS Chicherin (2020). proposed a control approach to monitoring the system substation valves based on the ambient temperature profile according to the cooling load prediction Gang et al. (2016). proposed a robust optimization control method for the DCS to relieve the system performance degradation caused by the maintenance failure of components or subsystems Zabala et al. (2020). developed a reliable model of a DCS containing compressors chillers and absorption chillers for the model predictive control optimization study. Simulation results showed that the application of model predictive control techniques could save up to 50% of the energy consumption compared to the baseline case.

Moreover, ice storage technology has been emphasized as one of the efficient load shifting techniques for the DCS (Kamal et al., 2019). A lot of research was carried out in terms of the thermal performance (Song et al., 2018a) configuration design (Tam et al., 2019), dispatch optimization (Lake et al., 2017), and economic feasibility (Song et al., 2018b) of the ice storage system integrated DCS (Heine et al., 2021). Increasing intelligent control method optimization for the district cooling integrated with thermal storage systems has been developed in recent research (Zhao et al., 2021). The artificial neural network-based model predictive control strategy was proposed by Coccia et al. (2021) for the DCS covering an eight-user residential neighborhood with a limited reference value for optimal control of the large-scale DCSs covering commercial and office buildings due to the entirely different building cooling load characteristics Yan et al. (2021). proposed an online multi-objective operation optimization strategy for the DCS, which took both energy consumption and thermal comfort within consideration, while the control strategy of the DSC integrated with thermal storage systems was more complicated than the separate DSC due to the dynamic cooling supply distribution of the chillers and thermal storage systems during time-of-use electricity prices. A neural network-based model predictive control strategy of the ice storage DCS was developed by Cox et al. (2019). It achieved effective operating cost-saving, in which the energy-saving performance of the variable-speed water pumps was not fully exploited since they were utilized as constant-speed water pumps in the proposed control method. However, current studies still pose some limitations for barely considering the complicated dynamic cooling supply distribution scenarios of the DCS and the thermal storage systems under different electricity tariffs.

To achieve demand-side management of grid operations (D'Ettorre et al., 2019), reduction of end-user energy consumption, and incorporation of renewable energy sources, systems combining heat pumps and thermal storage systems are common measures (Liu et al., 2021; Gelazanskas and Gamage, 2014), where the main control techniques that can be used to optimize the operation of energy storage systems in buildings include supervisory control, model predictive control (MPC) and machine learning control (Osterman and Stritih, 2021). The optimal control strategy has been extensively applied in all these studies (Baeten et al., 2017; Bechtel et al., 2020; Dar et al., 2014; Schibuola et al., 2015; Viot et al., 2018; Fischer et al., 2014) with promising optimization results, including optimization of COP for heat pumps (Meng et al., 2021) and optimization of thermal storage systems (Alimohammadisagvand et al., 2016; Arteconi et al., 2013; Fitzpatrick et al., 2020). The developed demand response control algorithms are all capable of reducing the delivered energy and operation costs compared to the baseline case, enabling peak and valley load reduction and flexible operation of the grid system. However, these studies mainly focused on the control optimization of air-source and ground-source heat pumps. At the same time, the water-energy storage and phase change energy storage were applied for the energy supply shift and flexible operation. The combinations of the ice storage system, water-source heat pump using rich river water, and large-scale district cooling system are still to be studied. The corresponding optimal control strategy is promisingly proposed for energy-saving and cost-saving.

Integrating low-temperature renewable energy sources such as geothermal energy, solar thermal energy, and waste heat into DHCS is expected to serve as an effective solution for reducing fossil fuel combustion and carbon emissions. At present, there are still some limitations of the existing studies on ice storage district cooling systems combined with renewable resources. At the same time, most of the current research focuses on the design optimization and control strategy of the ice storage systems and district cooling systems separately. Moreover, there are many practical limitations of single-building cooling load characteristics (mainly residential buildings) and failure to fully exploit the energy-saving advantages of variable-speed operation control strategies for water pumps and refrigerators of large-scale district cooling systems. Previous research proposed control strategies involved in the separate water temperature or flow rate control while combined water temperature and flow rate control have great potential for energy savings or operating cost savings (Mazzoni et al., 2021; Dorotić et al., 2019). Considering the complexity of the building load supply distribution schedule in different electricity price periods (Balboa-Fernández et al., 2020; Nouidui et al., 2019), how to implement intelligent control

optimization strategies to take the best advantage of the renewable energy sources and the thermal storage systems for achieving energy efficiency and cost-saving of the ice storage coupled with renewable energy sources district cooling system is still an urgent problem to be solved (Buffa et al., 2019; Sommer et al., 2020).

In this study, an integrated heat transfer model of the large-scale water-source heat pump coupled with an ice storage district cooling system was established, and experimental test data verified the accuracy of the developed model. Then the intelligent genetic algorithm (GA)-based optimal control strategy was proposed to take the most advantages of the district cooling system's water source energy and ice storage systems. The control variables and their constraints of the genetic algorithm (GA)-based optimal control strategy were identified through the comprehensive analysis of the test data. The objective function of the GA-based optimization control strategy of the water-source heat pump coupled with the ice storage district cooling system was developed by minimizing the operating cost per unit of the cooling supply. The economic and energy performance comparisons of the intelligent GA-based optimal control strategy, the ice melting priority strategy, and chiller priority were carried out to demonstrate the tremendous economic potential of the proposed intelligent control strategy.

2. Ice storage district cooling system description

The large-scale district heating and cooling system provided cooling and heating capacity for 2.44 million m^2 areas of public buildings, including office buildings, commercial buildings, hotels, etc., which take great advantage of the renewable river water resources and are integrated with advanced ice storage technology. A view of the three district zones and the location of the DCS is shown in Fig. 1.

The peak hourly cooling load of DCS was up to 187,516 kW at 15:00 on a typical summer design day, and the hourly cooling load and the load rate on a typical design day are shown in Fig. 2. The load rate was higher than 60% during the period of 10:00–18:00 and within the range of 35–60% during the periods of 8:00–9:00 and 19:00–21:00, while the load rate at other moments was around 10%, which was caused by the lower ambient temperature and the absence of solar radiation and occupants at night. The general information of the water-source heat pump integrated with the ice storage DSC and main equipment performance parameters are presented in Table 1. DCS adopts the combination operation of water-source heat pumps (WSHP), dual-mode water-source heat pumps (DMHP), and ice storage systems under the summer cooling condition. The winter heating conditions are not considered in this research since district heating and cooling systems are currently only used for summer cooling conditions.

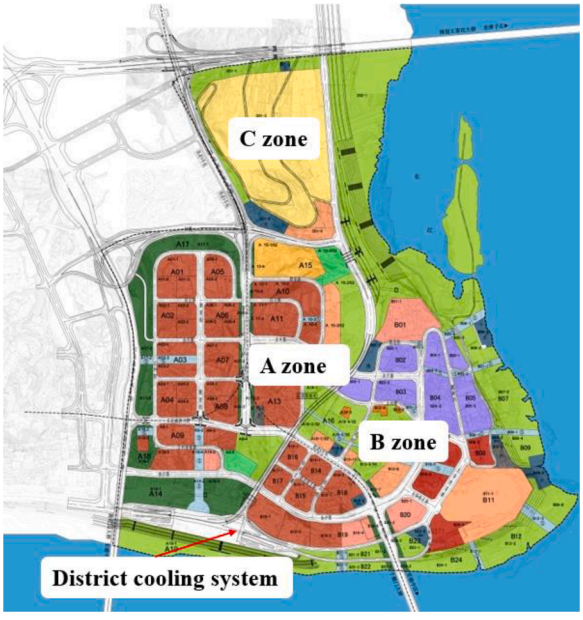

Fig. 1. A view of the three district zones and the location of the DCS.

Based on the design documents of the district cooling system and the under-construction and future planning of the area to be served, the daily hourly cooling load of the system in summer is calculated. After the initial selection of equipment, a better ratio of the ice storage system to the total cooling capacity of the system is finally selected according to the local power policy and the calculated initial investment, operating costs, and considering other factors. Therefore, the DCS is equipped with 18 cooling pieces of equipment, including 10 WSHPs for base heat load and 8 DMHPs, 320 ice storage coils with a total ice storage capacity of 33 GWh. Besides, 6 sets of plate-type heat exchangers for ice melting (PTHE (IM)) and 8 sets of plate-type heat exchangers for cooling (PTHE(COOL)) are installed.

The schematic diagram of the WSHP coupled with the ice storage DCS is presented in Fig. 3. The return water from the user side is cooled by WSHP and DMHP units first and then further cooled by the ice storage system while the chillers cannot afford to the cooling supply at the higher cooling load periods. During the night, the separate cooling mode of the WSHP is running while automatic loading or unloading of the WSHP according to the transient cooling load, and the ice storage mode of DMHP is activated at valley electricity price periods. Then a separate ice storage system for cooling supply mode runs in the daytime peak electricity price periods. At the same time, the WSHP takes priority for cooling supply followed by DMHP cooling supply mode in the lower electricity price periods of daylight. Based on the hourly forecast cooling load, the cooling supply ratio between WSHP/DMHP and the ice storage system is determined for more significant economic benefits at different electricity price periods.

3. Methodology

3.1. Model description

The simplified multivariate polynomial regression model (SMP model) (Wang, 2017) is identified as the mathematical model for capturing the dynamic characteristics of the WSHP and DMHP due to the incredible accuracy and simplified model configuration. The SMP model contains three essential independent variables of the cooling supply of the cooling unit Q_0, the chilled water supply temperature on the evaporation side T_{eo}, the cooling water return temperature on the condensation side T_{ci}, which is proposed after the multivariate polynomial model simplification based on performance parameter identification. The eight simplified parameters of the SMP model related to the dynamic properties of the WSHP and DMHP are obtained as presented in Eq. (1), which was proposed by Wang (2017) after simplifying the DOE model in Reddy and Andersen (2002).

$$COP = a0 + a1\cdot Q_0 + a2\cdot T_{eo} + a3\cdot T_{ci} + a4\cdot {Q_0}^2 + a5\cdot Q_0\cdot T_{eo} + a6\cdot Q_0\cdot T_{ci} + a7\cdot T_{eo}\cdot T_{ci} \quad (1)$$

Applying the test data of the WSHP based on the parameter identification method, the performance curve of the WSHP is obtained as:

$$COP_{WSHP} = -105.97 - 12.989\cdot Q_{WSHP} - 12.829\cdot T_{eo} + 1.11\cdot T_{ci} - 1.24 \times 10^{-6}\cdot {Q_{WSHP}}^2 + 0.0003\cdot Q_{WSHP}\cdot T_{eo} + 0.48182\cdot Q_{WSHP}\cdot T_{ci} + 0.37958\cdot T_{eo}\cdot T_{ci} \quad (2)$$

The relationship between the actual cooling supply Q_{WSHP} and the power consumption W_{WSHP} of a WSHP unit is described as follows.

$$Q_{WSHP} = C_w M_{WSHP}(T_{ci} - T_{eo}) \quad (3)$$

$$W_{WSHP} = \frac{Q_{WSHP}}{COP_{WSHP}} \quad (4)$$

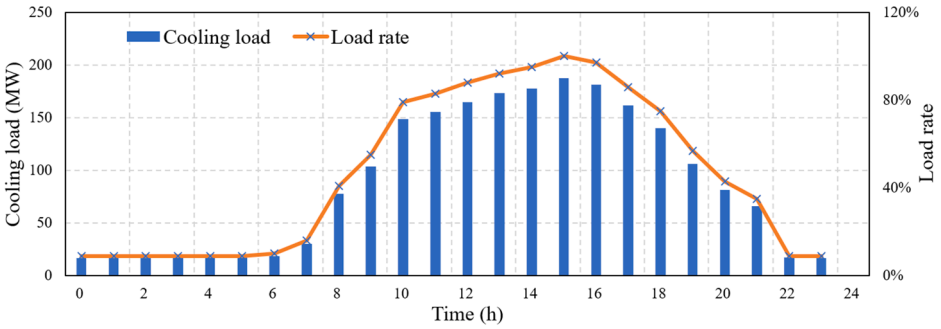

Fig. 2. . The hourly cooling load and the load rate on a typical design day.

Table 1.
General information of water-source heat pump integrated with the ice storage DSC and main equipment performance parameters.

Building function	Office, commercial, hotel, etc.				
Building area /m^2	2.44 million				
System type	District heating and cooling system integrated with ice storage system				
Peak cooling load /kW	187,516				
Main equipment	Water-source heat pump	Dual-mode heat pump	Ice storage coils	Heat exchanger	
Number	10	8	320	6	8
Cooling capacity /kW	8400	8545	/	6615	8544
Ice storage /kW	/	5043	/	/	/
Ice storage capacity /GWh	/	/	33	/	/

Similarly, the SMP model is selected as the mathematical model of the DMHP unit under the cooling mode, and its performance curve based on the parameter identification is identified as follows.

$$\begin{aligned} COP_{DMHP,\,COOL} = {} & -45.969 - 9.499\cdot Q_{DMHP,\,COOL} - 8.075\cdot T_{geo} + 0.191\cdot T_{ci} \\ & - 3.356 \times 10^{-6}\cdot Q_{DMHP,\,COOL}{}^{2} - 2.000\cdot Q_{DMHP,\,COOL}\cdot T_{geo} \\ & + 0.611\cdot Q_{DMHP,\,COOL}\cdot T_{ci} + 0.776\cdot T_{geo}\cdot T_{ci} \end{aligned} \tag{5}$$

Besides, the actual cooling supply $Q_{DMHP,\,COOL}$ and the power consumption $W_{DMHP,\,COOL}$ of the DMHP unit under cooling mode can be obtained.

$$Q_{DMHP,\,COOL} = C_g M_g (T_{gei} - T_{geo}) \tag{6}$$

$$W_{DMHP,\,COOL} = \frac{Q_{DMHP,\,COOL}}{COP_{DMHP,\,COOL}} \tag{7}$$

The ice storage mode of the DMHP unit is turned on from 23:00 to 7:00 at night, and the ice storage model of the DMHP unit is described by the characteristic curve of $COP_{DMHP,\,IS}$ on partial load rate PLR, which indicates the ratio of the cooling supply to the maximum cooling capacity based on the improved DOE-2 model.

$$COP_{DMHP,IS} = \begin{cases} 1.4072 + 6.1532.PLR - 3.0712.PLR^2, & 0.5 \le PLR \le 1 \\ 1.6178 + 12.687.PLR - 12.175.PLR^2, & 0.1 \le PLR \le 0.5 \end{cases} \tag{8}$$

$$Q_{DMHP,\,IS} = C_g M_g (T_{bei} - T_{beo}) \tag{9}$$

$$W_{DMHP,\,IS} = \frac{Q_{DMHP,\,IS}}{COP_{DMHP,\,IS}} \tag{10}$$

The hydraulic system on the condensation side is running at constant frequency to reduce the negative impact on the cooling performance caused by the river water flow rate fluctuation. The power consumption curves of the water pumps on the condensation side of the WSHP and DMHP are obtained as follows.

$$\begin{cases} W_b = 2.6612 + 3 \times 10^{-7}M^3 - 0.0003M^2 + 0.1619M \\ W_{BS} = 27.226 - 2 \times 10^{-7}M^3 + 0.0001M^2 - 0.0182M \\ W_{BQ} = 72.017 - 5 \times 10^{-9}M^3 + 6 \times 10^{-6}M^2 + 0.0292M \end{cases} \tag{11}$$

The DCS adopts the primary-secondary chilled water systems with primary water pumps on the WSHP and DMHP side and secondary water pumps on the user side since higher water pump pressure will be required for the long-distance water transmission and distribution system. All primary and secondary chilled water heat pumps run under variable speed conditions. The head-flowrate characteristic curves for water pumps in parallel operation at variable speed ratio k are demonstrated as follows, respectively. And i is the number of water pumps.

$$\begin{cases} \mathbf{H_B} = -7 \times 10^{-6}(\mathbf{M/i})^2 - 0.0002\cdot\mathbf{k}\cdot\mathbf{M}/\mathbf{i} + 18.766\cdot\mathbf{k}^2 \\ \mathbf{H_{BY}} = -6 \times 10^{-6}(\mathbf{M/i})^2 - 0.002\cdot\mathbf{k}\cdot\mathbf{M}/\mathbf{i} + 40.363\cdot\mathbf{k}^2 \\ \mathbf{H_{B1}} = 4 \times 10^{-6}(\mathbf{M/i})^2 - 0.0062\cdot\mathbf{k}\cdot\mathbf{M}/\mathbf{i} + 25.394\cdot\mathbf{k}^2 \\ \mathbf{H_{Br}} = -8 \times 10^{-7}(\mathbf{M/i})^2 - 0.0015\cdot\mathbf{k}\cdot\mathbf{M}/\mathbf{i} + 24.819\cdot\mathbf{k}^2 \\ \mathbf{H_{B2}} = -3 \times 10^{-6}(\mathbf{M/i})^2 - 0.0041\cdot\mathbf{k}\cdot\mathbf{M}/\mathbf{i} + 92.76\cdot\mathbf{k}^2 \end{cases} \tag{12}$$

The energy efficiency-flowrate characteristic curves of the water pumps in parallel operation at variable speed ratio k are presented as follows.

$$\begin{cases} \eta_{\mathbf{B}} = -8 \times 10^{-11} \times \mathbf{k}^{-3} \times (\mathbf{M/i})^3 - 8 \times 10^{-7} \times \mathbf{k}^{-2} \times (\mathbf{M/i})^2 + 0.0017 \times \mathbf{k}^{-1} \times \mathbf{M}/\mathbf{i} \\ \eta_{\mathbf{BY}} = 5 \times 10^{-11} \times \mathbf{k}^{-3} \times (\mathbf{M/i})^3 - 5 \times 10^{-7} \times \mathbf{k}^{-2} \times (\mathbf{M/i})^2 + 0.0012 \times \mathbf{k}^{-1} \times \mathbf{M}/\mathbf{i} \\ \eta_{\mathbf{B1}} = -1 \times 10^{-12} \times \mathbf{k}^{-3} \times (\mathbf{M/i})^3 - 4 \times 10^{-7} \times \mathbf{k}^{-2} \times (\mathbf{M/i})^2 + 0.0012 \times \mathbf{k}^{-1} \times \mathbf{M}/\mathbf{i} \\ \eta_{\mathbf{Br}} = 2 \times 10^{-11} \times \mathbf{k}^{-3} \times (\mathbf{M/i})^3 - 2 \times 10^{-7} \times \mathbf{k}^{-2} \times (\mathbf{M/i})^2 + 0.0008 \times \mathbf{k}^{-1} \times \mathbf{M}/\mathbf{i} \\ \eta_{\mathbf{B2}} = 3 \times 10^{-11} \times \mathbf{k}^{-3} \times (\mathbf{M/i})^3 - 3 \times 10^{-7} \times \mathbf{k}^{-2} \times (\mathbf{M/i})^2 + 0.0008 \times \mathbf{k}^{-1} \times \mathbf{M}/\mathbf{i} \end{cases} \tag{13}$$

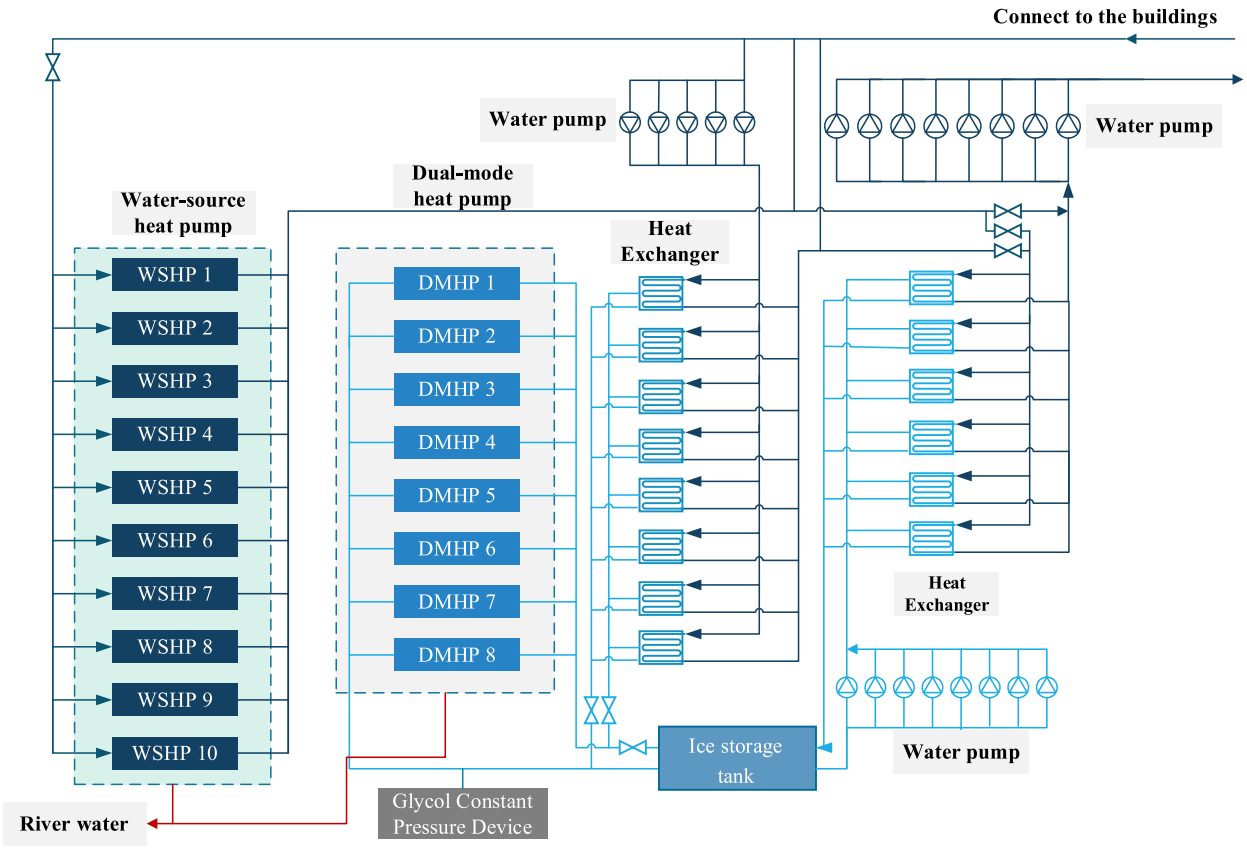

Fig. 3. Schematic diagram of the WSHP coupled with ice storage district cooling system.

The typical energy efficiency regression curves for motors and inverters of water pumps are shown as follows (Ashrae, 2018).

$$\eta_m = 0.94187\left(1 - e^{-9.04k}\right) \tag{14}$$

$$\eta_f = 1.2833k - 1.42k^2 + 0.5482k^3 + 0.5067 \tag{15}$$

In turn, the power consumption of each water pump can be obtained as follows.

$$w = \frac{\rho gHM}{1000\eta\eta_m\eta_f} \tag{16}$$

The ice storage system needs to ensure that the water supply temperature of the DCS is at the design value of 3 °C by adjusting the ice melt ratio. The ice storage system can supply cooling steadily and maintain a water supply temperature of 0.25 °C when the ice melting ratio β (the percentage of melted ice to total ice storage) is lower than 65%. The water supply temperature rises rapidly with the increase of β, and the final water supply temperature reaches 3.1 °C while β reaches more than 80%. The ice storage system in this research can provide a stable water supply temperature range between 0.25 and 3.1 °C and the water supply temperature is close to the water return temperature of up to 3.2 °C when β exceeds 97.5%. Based on the empirical test data and the performance parameter identifications of the ice storage equipment, the performance curve of the water supply temperature T_{geo} of the ice storage system with β can be fitted as follows.

$$\mathbf{T_{geo}} = 0.31048 + 0.00277\cdot\mathbf{e}^{6.8936\cdot\beta} \tag{17}$$

For the sake of model simplification, the average water supply temperature of the ice storage system is taken as 1.5 °C according to the determination criterion for stable heat exchange according to the design description of the ice storage coils and the actual operation data. The expression of β of the ice storage system versus the time variable t can be obtained as follows.

$$\beta = 1.1992 - 1.3176\cdot\mathbf{e}^{-0.11106\cdot t} \tag{18}$$

In turn, the expression for the ice melting rate ε (melted ice volume per unit time) can be obtained by deriving the above equation for time.

$$\varepsilon(\beta) = \mathbf{d}\beta/\mathbf{dt} = 0.1463 \times (1.1992 - \beta)/1.3176 \tag{19}$$

The discharge capacity δ indicated by the adequate cooling supply proportion to the maximum cooling capacity provided by the ice storage system can be fitted as follows according to the above theoretical models.

$$\delta = \frac{\mathbf{Q_{cooling}}}{\mathbf{Q_{ice\ storage}}} = 96.10\% \tag{20}$$

3.2. DCS model validation

The heat transfer model of the WSHP coupled with the ice storage DCS was established in the TRNSYS environment, as shown in Fig. 4. The heat transfer process and the control system design are relatively more complicated because of the large-scale DCS system integrated with advanced ice storage systems and renewable river water sources, providing a theoretical reference for the control strategy optimization study of the ice storage district cooling system applying renewable energy sources.

The experimental operation data of the DCS on August 11, 2020, was selected for model validation. The measurement parameters such as the river water supply ambient temperature hourly cooling load were set as the boundary conditions of simulation models. The DMHP unit was used for ice storage from 00:00 to 7:00, and then the ice storage system was applied for cooling supply for daytime. The WHSP was used for supplementary cooling supply as the ice storage system during the day. The total energy consumption of the DCS included the power consumptions

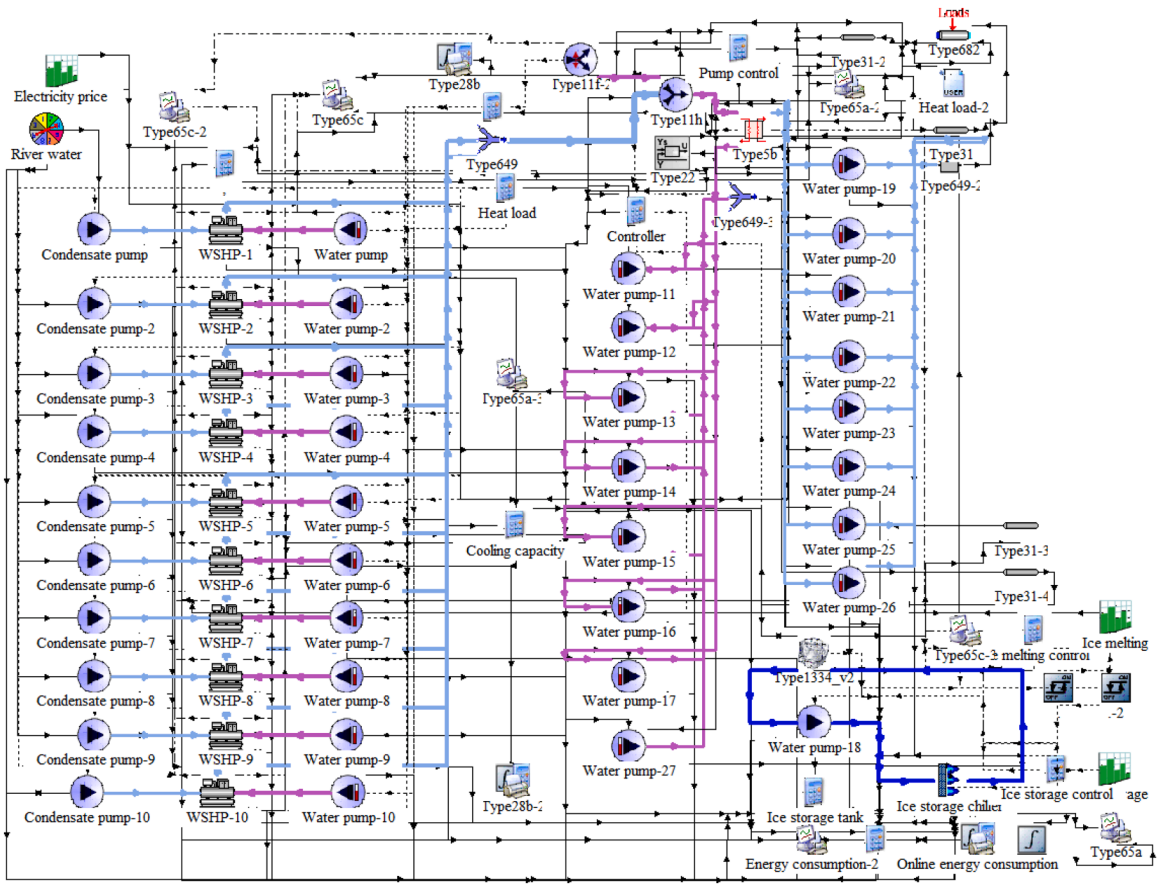

Fig. 4. The simulation model of the WSHP coupled with ice storage district cooling system in the TRNSYS environment.

of the DMHP unit, the WSHP unit, and all the primary and secondary water pumps. The simulation and experimental results comparisons of the power consumption of the DMHP unit, the WSHP unit, the water pumps, and the total power consumption of the DCS are shown in Fig. 5.

The power consumption trends of the main equipment obtained from the simulation models were generally consistent with those of the experimental measurement results. Overall, the simulated total power consumption was slightly lower than the experimental one, caused by the heat loss of the water distribution systems and the heat exchange loss between experimental components in the practical operation that was ignored in the simulation for simplification. The relative error of the power consumptions of the DMHP unit, the WHSP unit, and the water pumps for 24 h was 9.28% on average between the simulation and experimental results, which was less than 10% of the power consumption validation standards and criteria (Ciulla and D'Amico, 2019). Therefore, the DCS model's accuracy has been validated and can be effectively applied for the following control strategy optimization research.

3.3. Control strategy optimization based on GA

For the intelligent control strategy optimization of the nonlinear air conditioning systems, the commonly used algorithms mainly include genetic algorithm (GA), particle swarm algorithm, and simulated annealing algorithm. These three main algorithms are highly applicable to large-scale nonlinear optimization problems. Genetic algorithm is applied chiefly to the global optimization problem because of its excellent global search capability. This study will further investigate the control strategy optimization of the WSHP coupled with ice storage DCS based on GA for reasonable cooling supply distribution and better cost-effectiveness. And its energy performance and running cost will be compared with the commonly used control strategies under typical cooling load conditions. The control strategy optimization of the DCS requires the operation scheduling optimization of the WSHP, the DMHP, and the ice storage system for reducing operating energy consumption compared with the conventional control strategy of DCSs and the overall operational cost trade-off combined with the time-of-use tariff policy should be taken into serious consideration.

The DCS has these main operating modes: ice storage mode, the WSHP for cooling, the DMHP for cooling, the WSHP and DMHP for cooling, the ice storage system for cooling, and the combined cooling supply of the WSHP, DMHP, and ice storage system. To minimize the overall operating cost of the system, the DCS needs to take the best advantage of the electricity prices at peak and valley periods and implement the cost-effective cooling supply scenarios of the ice storage system as soon as possible while meeting the building's cooling demand. The DCS was running at partial load most of the time, while the practical cooling load was generally only about 40% ~ 80% of the design cooling load. The proportion of the cooling supply by the ice storage system to the total cooling supply of the DCS is defined as the ice melting cooling ratio γ demonstrated as follows. Therefore, the control strategy optimization of the DCS depends on the optimal schedule of the ice melting cooling ratio γ at peak and valley electricity price periods.

$$\gamma = \frac{\mathbf{q}_{\mathbf{DMHP,\ IS}}}{\mathbf{q}_{\mathbf{t}}} \tag{21}$$

The relationships among the total cooling supply $\mathbf{q}_{\mathbf{t}}$, the cooling supply of the WSHP unit $\mathbf{q}_{\mathbf{WSHP}}$, the cooling supply of the DMHP unit $\mathbf{q}_{\mathbf{DMHP}}$, and the cooling supply of the ice storage system $\mathbf{q}_{\mathbf{DMHP,\ IS}}$ can be simplified with the indicators of the ice melting cooling ratio γ and the cooling supply proportion θ of the WSHP unit to the total cooling supply of the DCS. The two parameters γ and θ are independent of each other.

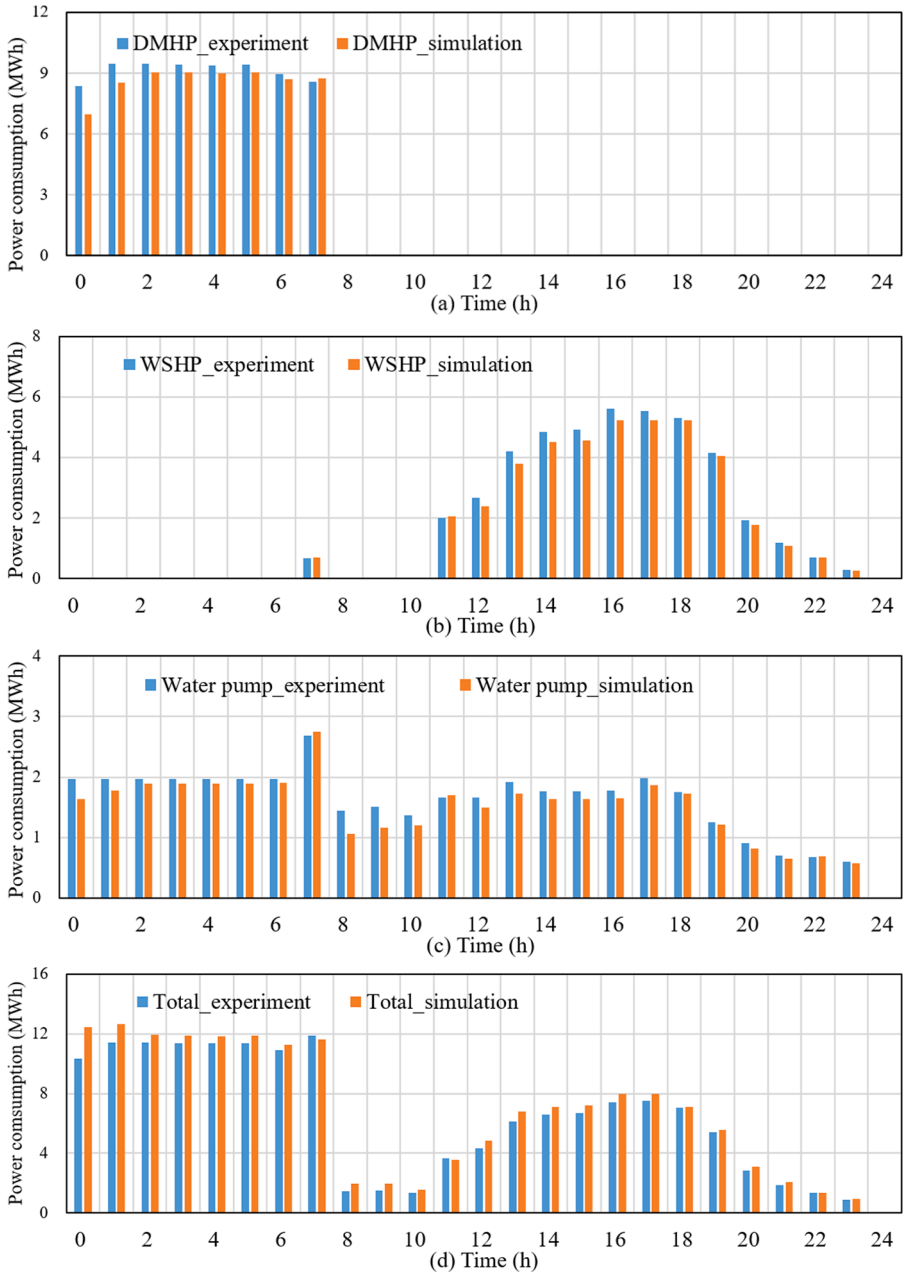

Fig. 5. The simulation and experimental results comparisons of the power consumptions of (a) the DMHP unit, (b) the WSHP unit, (c) the water pumps, and (d) the total power consumption of the DCS.

$$\begin{cases} \mathbf{q}_{\mathbf{DMHP,\ IS}} = \mathbf{q_t} \cdot \gamma \\ \mathbf{q}_{\mathbf{WSHP}} = \mathbf{q_t} \cdot \theta \\ \mathbf{q}_{\mathbf{DMHP,\ COOL}} = \mathbf{q_t} \cdot 1 - \gamma - \theta \end{cases} \tag{22}$$

The water temperature or flow rate control strategy was primarily applied in previous research, while the temperature-flowrate combined control strategy can achieve better energy efficiency and economic benefits for the DCS. and the parameters of γ, θ will. Therefore, the three independent variables of γ, θ, controlled by the variable-speed water flowrate control and the water supply temperature $\mathbf{T}_{\mathbf{ws}}$ of the WSHP and DMHP are finally identified as the control variables of the intelligent optimal control strategy based on GA for the DCS in this research. Taking the peak and valley electric charges in Chongqing as an example demonstrated below, the system's objective function operating cost per unit of cooling supply for a single day is established as follows.

$$\begin{cases} min(J) = \dfrac{\mathbf{E}}{\mathbf{Q_t}} = \dfrac{\sum_{t=0}^{23} \left\{ \left[\mathbf{W}_{\mathbf{WSHP}}(\mathbf{t}) + \mathbf{W}_{\mathbf{DMHP,\ COOL}}(\mathbf{t}) + \mathbf{W}_{\mathbf{DMHP,\ IS}}(\mathbf{t}) + \mathbf{W}_{\mathbf{p}}(\mathbf{t}) \right] \cdot \mathbf{e}(\mathbf{t}) \right\}}{\mathbf{Q_t}} \\ S \end{cases} \tag{23}$$

$$\mathbf{e(t)}=\begin{cases}0.3466, t=23\sim 6\\ 0.6932, t=7,\ 12\sim 18\\ 1.0398, t=8\sim 11,\ 21\sim 22\\ 1.1784, t=19,\ 20\end{cases} \tag{24}$$

The objective function **J** represents the operating cost per unit of cooling supply, **CNY/kWh.** E is the operating cost of the DCS for a single day, CNY. $\mathbf{Q_t}$ is the total cooling supply provided by the WSHP, the DMHP, and the ice storage system for a single day, **kW·h**. e(t) is the electricity price at different periods, **CNY/kW·h**. S is the operating parameters constraints of the DCS.

The total energy consumption of all the water pumps $\mathbf{W_p(t)}$ is expressed as.

$$\mathbf{W_p(t)}=\mathbf{W_{pB}(t)}+\mathbf{W_{pb}(t)}+\mathbf{W_{pBY}(t)}+\mathbf{W_{pBS}(t)}+\mathbf{W_{pBr}(t)}+\mathbf{W_{pB2}(t)}+\mathbf{W_{pBQ}(t)}+\mathbf{W_{pB1}(t)} \tag{25}$$

Considering the practical cooling demand from the user side, the total water supply temperature of the DCS needs to be controlled to be 4.5 °C and 3 °C during the ice storage period and the cooling supply period, respectively. The total water supply temperature $\mathbf{T_{tws}(t)}$ can be summarized below.

$$\mathbf{T_{tws}(t)}=\begin{cases}4.5, t=23-6\\ 3,\ t=7-23\end{cases} \tag{26}$$

The cooling supply rate PLR of the WSHP and DMHP should be ensured to be between 25 and 100% to maintain the stable system operation.

$$25\%\le \mathbf{PLR}\le 100\% \tag{27}$$

The flow rate of the water pumps should be ensured at more than 30% of the rated flow rate for avoiding inefficient operation at low speed.

$$30\%\mathbf{m_o}\le \mathbf{m}\le \mathbf{m_o} \tag{28}$$

Where $\mathbf{m_o}$ and $\mathbf{m}$ are the rated and practical flowrate of water pumps, $\mathbf{m^3/h}$.

The total ice storage volume $\mathbf{Q_{DMHP,IS,\ total}}$ should not exceed the maximum capacity of the ice storage tank $\mathbf{Q_{DMHP,IS,max}}$ and the daily melted ice volume for cooling $\mathbf{Q_{IS}}$ should be more than 95% of the total ice storage volume $\mathbf{Q_{DMHP,IS,total}}$ for a single day.

$$0\le \mathbf{Q_{DMHP,IS,total}}\le \mathbf{Q_{DMHP,IS,max}} \tag{29}$$

$$\mathbf{Q_{DMHP,IS,total}}\cdot\delta\cdot 95\%\le \mathbf{Q_{DMHP,IS}}\le \mathbf{Q_{DMHP,IS,total}}\cdot\delta \tag{30}$$

The instantaneous cooling supply should be lower than the maximum limitation, and $\varepsilon(\beta)$ represents the ice melting ratio.

$$\mathbf{q_{DMHP,\ IS}t}\le \varepsilon\beta\cdot\mathbf{Q_{DMHP,IS,total}} \tag{31}$$

The water supply temperature of the WSHP and DMHP is constrained among the below range.

$$\mathbf{T_{ws}}\in(3\sim 7)^{\circ}\mathrm{C} \tag{32}$$

The cooling supply balance and the water flowrate balance of the DCS should be maintained as the following equations described. $\mathbf{m_{WSHP}}$, $\mathbf{m_{DMHP}}$, and $\mathbf{m_{DMHP,\ IS}}$ are the return water flowrates that transfer heat with the WSHP, the DMHP, and the ice storage system.

$$\begin{cases}\mathbf{q_t(t)}=\mathbf{q_{WSHP}(t)}+\mathbf{q_{DMHP,\ COOL}(t)}+\mathbf{q_{DMHP,\ IS}(t)}\\ 0\le\gamma\le 1\\ 0\le\theta\le 1\end{cases} \tag{33}$$

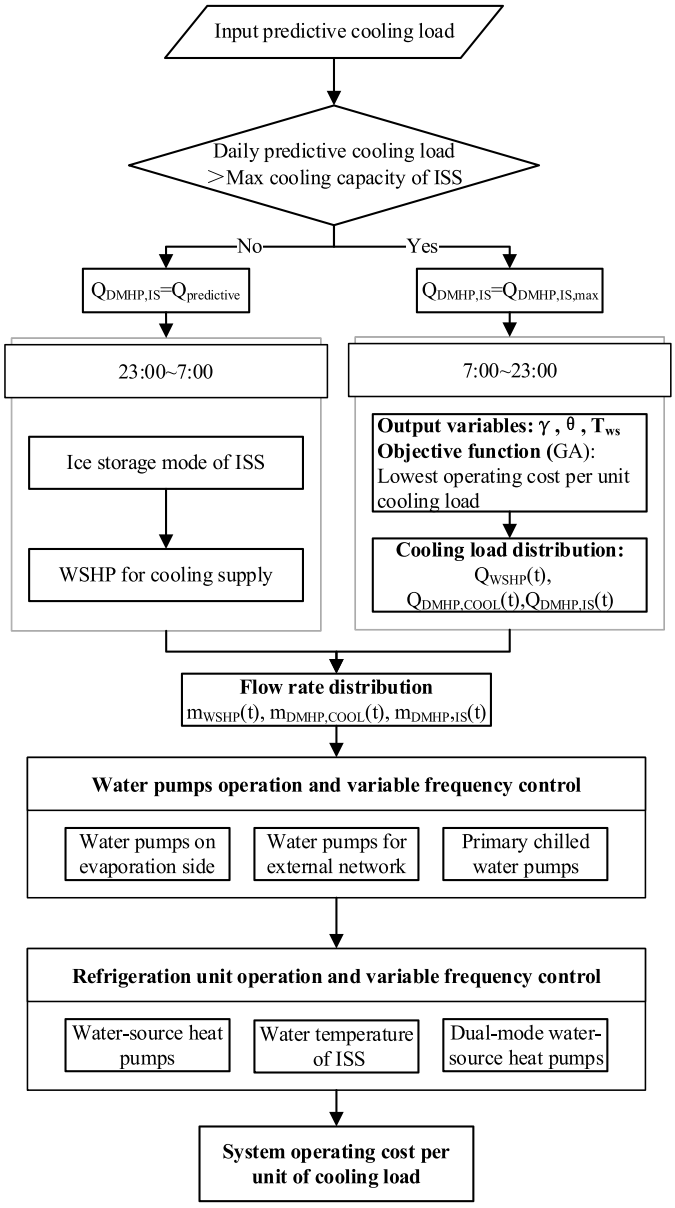

Fig. 6. The flow chart of the control strategy optimization of the WSHP coupled with ice storage district cooling systems based on GA.

$$\begin{aligned}\mathbf{Q_t}&=\mathbf{Q_{WSHP}}+\mathbf{Q_{DMHP,\ COOL}}+\mathbf{Q_{DMHP,\ IS}}\\ \mathbf{Q_{WSHP}}&=\sum_{t=0}^{24}\mathbf{q_{WSHP}(t)}\\ \mathbf{Q_{DMHP,\ COOL}}&=\sum_{\mathbf{t}=0}^{24}\mathbf{q_{DMHP,\ COOL}(t)}\\ \mathbf{Q_{DMHP,\ IS}}&=\sum_{t=0}^{24}\mathbf{q_{DMHP,\ IS}(t)}\end{aligned} \tag{34}$$

$$\begin{aligned}\mathbf{m_t(t)}&=\mathbf{m_{WSHP}(t)}+\mathbf{m_{DMHP,\ COOL}(t)}+\mathbf{m_{DMHP,\ IS}(t)}\\ 0&\le\mathbf{m_{WSHP}(t)}\le\mathbf{m_t(t)}\\ 0&\le\mathbf{m_{DMHP,\ COOL}(t)}\le\mathbf{m_t(t)}\\ 0&\le\mathbf{m_{DMHP,\ IS}(t)}\le\mathbf{m_t(t)}\\ 0&\le\mathbf{m_t(t)}\end{aligned} \tag{35}$$

The objective function and parameter constraints for the control strategy optimization based on GA are introduced above. In this research, the population size was set to 3000 to ensure the optimal solution's accuracy. The crossover fraction was set to 0.8, and the

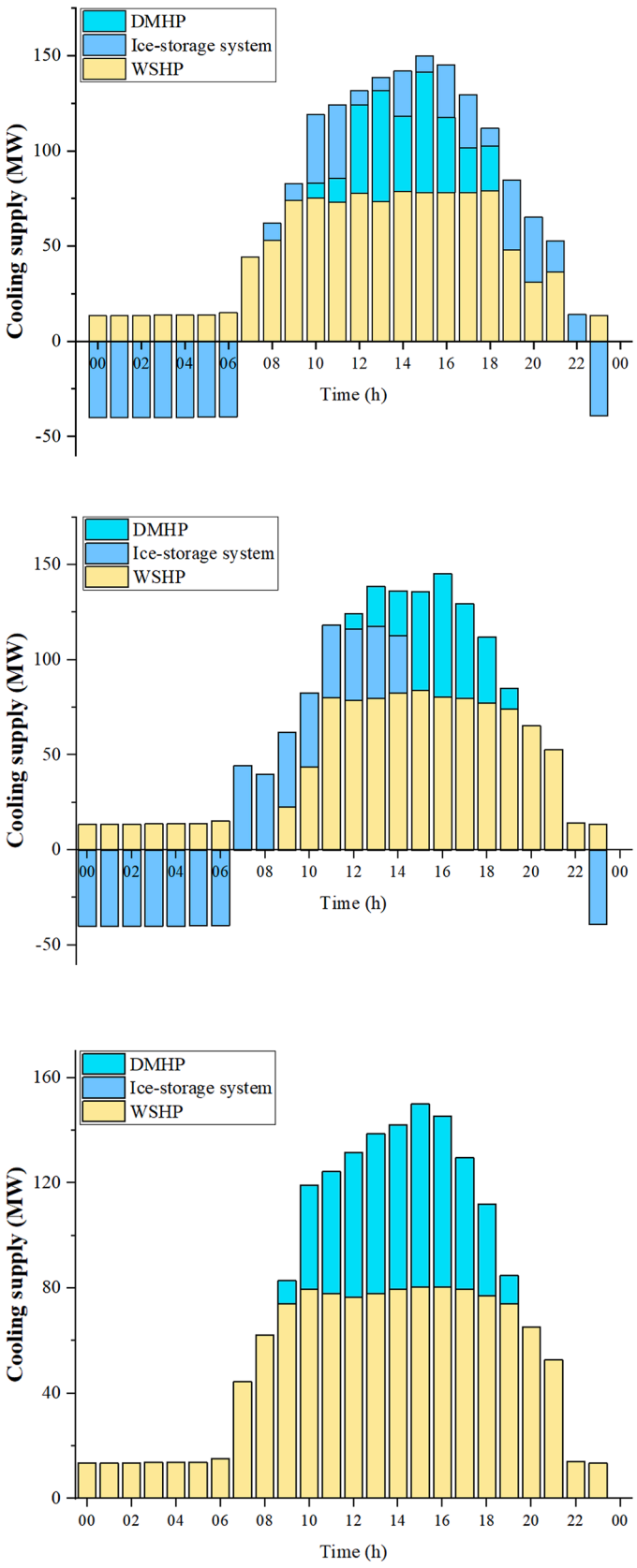

Fig. 7. The cooling supply distributions of DCS under the GA-based optimal control strategy, the ice melting priority control strategy, and the WSHP priority control strategy at about 80% of the design cooling load. (a) GA-based optimal control strategy. (b) Ice melting priority. (c) WSHP priority.

mutation fraction was set to 0.1. According to the iterative termination criteria, the maximum generation number was set to 300. The flowchart of the control strategy optimization of the WSHP coupled with ice storage district cooling systems based on GA is presented in Fig. 6. The ice storage volume is identified according to the forecast cooling load in advance. Then the control variables of γ, θ, and $\mathbf{T}_{ws}$ of the WSHP and DMHP are obtained by minimizing the objective function based on GA. And the cooling supply distributions of the WSHP, the DMHP, and the ice storage system are identified at different electricity price periods. Moreover, the water pumps' flow rate and variable speed control are conducted. The operation numbers and frequency control of the WSHP and DMHP units are carried out to supply the demanded cooling.

4. Results and discussion

The simulation results of the proposed optimal control strategy based on GA, the conventional ice melting priority strategy, and the WSHP priority strategy for the DCS were obtained under 80% of the daily design cooling load. The ice melting priority strategy means that the WSHP and DMHP units are not used for cooling supply until the ice storage is exhausted, while the WSHP priority strategy indicates that the DMHP units and the ice storage system are not applied for cooling supply until the WSHP cannot afford the cooling demand. The three control strategies' energy consumption and operating cost performance will be further evaluated and compared.

According to the GA-based optimal control strategy, the optimized water supply temperature setting value of the WSHP and DMHP units was determined to be 3.5 °C during the non-valley electricity price periods. The cooling supply distribution of the DCS under the GA-based optimal control strategy at 80% of the design cooling load is shown in Fig. 7(a). The ice storage tank was running at nearly full capacity due to the more considerable cooling demand during the valley electricity price periods of 23:00–7:00, while two WSHP units carried out the cooling supply at night. The DMHP units were turned on into operation for cooling supply from 10:00 to 18:00 when the WSHP units and the ice storage system could not afford the increased cooling demand. The ice storage system was running at nearly the maximum ice melting rate to reduce the operating cost in the peak hours of 8:00–12:00. During the peak periods of 19:00–23:00, the cooling supply was shared by the ice storage system and the WSHP units. Only the ice storage system was separately used for cooling supply at 23:00 when the cooling demand was lower. The increasing cooling demand led to the more significant

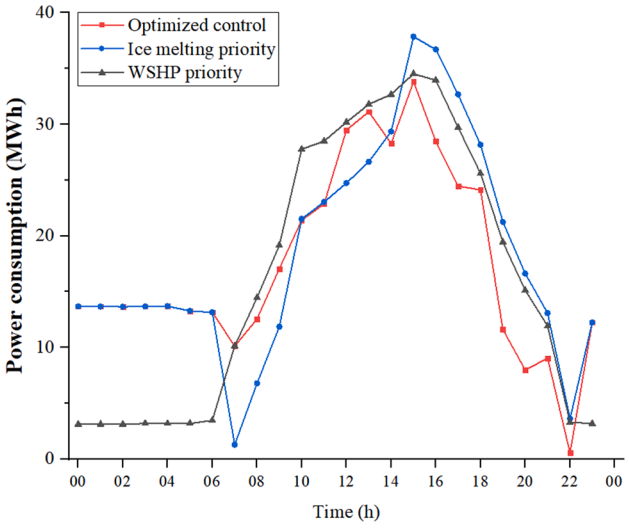

Fig. 8. The power consumptions of the DCS under the GA-based optimal control strategy, the ice melting priority control strategy, and the WSHP priority control strategy at 80% of the design cooling load.

Table 2.
The operating costs comparison under the GA-based optimal control strategy, the ice melting priority control strategy, and the WSHP priority control strategy at 80% of the design cooling load.

Time	Total operating costs (CNY)		
	GA-based optimized control strategy	Conventional control strategy	
		Ice melting priority	WSHP priority
Valley period (23:00–7:00)	37,105	37,103	8876
Flat period (7:00–8:00, 12:00–19:00)	145,521	150,681	158,441
Peak period (8:00–12:00, 21:00–23:00)	84,711	83,081	109,285
Sharp period (19:00–21:00)	23,091	44,626	40,739
Total	287,228	312,385	314,306
Operating cost per unit cooling load (**CNY**/**kW**)	0.172	0.187	0.188
Operating cost savings ratio	/	8.7%	9.3%

stored ice consumption in the daytime, leaving less residual stored ice in the ice storage tank for the peak hours at night.

The cooling supply distributions of the DCS under the ice melting priority control strategy and the WSHP priority control strategy at 80% of the design cooling load are shown in Fig. 7(b) and (c). The water supply temperature of the WSHP and the DMHP unit was set at 4.5 °C for both control strategies. The DMHP units were turned on for cooling supply from noon when the ice storage system was at its maximum ice melting rate, and the WSHP units could not afford the cooling demand. The ice storage was exhausted at 14:00 under the ice melting priority control strategy. Therefore, the cooling supply was shared by the WSHP and DMHP units in the subsequent hours. The peak ice melting rate was 51.0% under the ice melting priority control strategy, while it was increased to 63.4% under the GA-based optimal control strategy. The WSHP units combined with the DMHP units for cooling supply were required most of the time under the WSHP priority strategy due to the higher 80% cooling demand.

The power consumptions of the DCS under the GA-based optimal control strategy, the ice melting priority control strategy, and the WSHP priority control strategy at 80% of the design cooling load are shown in Fig. 8. The GA-based optimal control strategy had the lowest power consumption compared with the other control strategy after 15:00. It reduced the power consumption by 7.0% compared to the ice melting priority control strategy. Overall, the WSHP priority control strategy still had the lowest power consumption, followed by the GA-based optimal control strategy and the ice melting priority control strategy. The operating costs comparison under the GA-based optimal control strategy, the ice melting priority control strategy, and the WSHP priority control strategy at 80% of the design cooling load is presented in Table 2. In terms of the overall daily operating cost, the cost-saving percentage of the GA-based optimal control strategy was 8.7 and 9.3% compared with the ice melting priority control strategy and the WSHP priority control strategy, which demonstrated the excellent cost-effective performance of the GA-based optimal control strategy under higher cooling demand conditions.

5. Conclusion

In this study, a GA-based techno-economic optimal control strategy is proposed for a water-source heat pump coupled with an ice storage district cooling system which can effectively achieve economic and efficient operation. The proposed intelligent control approach applied the three independent control variables of the ice melting cooling ratio of the ice storage system, the water supply temperature, and the cooling supply proportion of the WSHP unit. The control parameters can be determined by addressing the minimum solution of the objective function of the operating cost per unit of cooling supply based on the genetic algorithm. An integerated heat transfer model of the water-source heat pump coupled with the ice storage district cooling system composed of 10 WSHP units, 8 DMHP units, and the ice storage system with 320 cooling coils was developed, and experimental test data verified its accuracy. The economic and energy performance comparisons of the GA-based optimal control strategy, the ice melting priority control strategy, and the WSHP priority control strategy were carried out at different cooling demand conditions. The WSHP priority control strategy had the best power consumption saving potential for the water-source heat pump coupled with the ice storage district cooling system compared with the other two control strategies. However, the simulation results demonstrated that the GA-based optimal control strategy could save 8.7–9.3% of operating costs compared with the ice melting priority control strategy and the WSHP priority control strategy under 80% cooling demands while maintaining the comparative energy-saving performance, which has confirmed the significant economic benefits of the proposed GA-based optimal control strategy for the water-source heat pump coupled with ice storage district cooling system.

Declaration of Competing Interest

We declare that we have no financial and personal relationships with other people or organizations that can inappropriately influence our work, there is no professional or other personal interest of any nature or kind in any product, service and/or company that could be construed as influencing the position presented in, or the review of, the manuscript entitled.

Reference

Xu, Y., Yan, C., Liu, H., et al., 2020. Smart energy systems: a critical review on design and operation optimization. Sustain. Cities Soc. 62, 102369.
Allen, A., Henze, G., Baker, K., et al., 2020. Evaluation of low-exergy heating and cooling systems and topology optimization for deep energy savings at the urban district level. Energy Convers. Manag. 222, 113106.
Wang, Y., Wang, Z., Wang, Z., 2021a. A stochastic load demand-oriented synergetic optimal control strategy for variable-speed pumps in residential district heating or cooling systems. Energy Build. 238, 110853.
Sun, F., Li, J., Fu, L., et al., 2020. New configurations of district heating and cooling system based on absorption and compression chillers driven by waste heat of flue gas from coke ovens. Energy 193, 116707.
Wang, Y., Zhang, S., Chow, D., et al., 2021b. Evaluation and optimization of district energy network performance: present and future. Renew. Sustain. Energy Rev. 139, 110577.
Alajmi, A., Zedan, M., 2020. Energy, cost, and environmental analysis of individuals and district cooling systems for a new residential city. Sustain. Cities Soc. 54, 101976.
Inayat, A., Raza, M., 2019. District cooling system via renewable energy sources: a review. Renew. Sustain. Energy Rev. 107, 360–373.
Han, K., Ji, J., Cai, J., et al., 2021. Experimental and numerical investigation on a novel photovoltaic direct-driven ice storage air-conditioning system. Renew. Energy 172, 514–528.
Deng, N., He, G., Gao, Y., et al., 2017. Comparative analysis of optimal operation strategies for district heating and cooling system based on design and actual load. Appl. Energy 205, 577–588.
Anderson, A., Rezaie, B., Rosen, M.A., 2021. An innovative approach to enhance sustainability of a district cooling system by adjusting cold thermal storage and chiller operation. Energy 214, 118949.
Abugabbara, M., Javed, S., Bagge, H., et al., 2020. Bibliographic analysis of the recent advancements in modeling and co-simulating the fifth-generation district heating and cooling systems. Energy Build. 224, 110260.
Falay, B., Schweiger, G., O'donovan, K., et al., 2020. Enabling large-scale dynamic simulations and reducing model complexity of district heating and cooling systems by aggregation. Energy 209, 118410.
Coccia, G., Mugnini, A., Polonara, F., et al., 2021. Artificial-neural-network-based model predictive control to exploit energy flexibility in multi-energy systems comprising district cooling. Energy 222, 119958.
Chan, A.L.S., Hanby, V.I., Chow, T.T., 2007. Optimization of distribution piping network in district cooling system using genetic algorithm with local search. Energy Convers. Manag. 48, 2622–2629.
Chiam, Z., Easwaran, A., Mouquet, D., et al., 2019. A hierarchical framework for holistic optimization of the operations of district cooling systems. Appl. Energy 239, 23–40.
Kang, J., Wang, S., Yan, C., 2019. A new distributed energy system configuration for cooling dominated districts and the performance assessment based on real site measurements. Renew. Energy 131, 390–403.

Chicherin, S., 2020. Methodology for analyzing operation data for optimum district heating (DH) system design: ten-year data of Omsk, Russia. Energy 211, 118603.
Gang, W., Wang, S., Augenbroe, G., et al., 2016. Robust optimal design of district cooling systems and the impacts of uncertainty and reliability. Energy Build. 122, 11–22.
Zabala, L., Febres, J., Sterling, R., et al., 2020. Virtual testbed for model predictive control development in district cooling systems. Renew. Sustain. Energy Rev. 129, 109920.
Kamal, R., Moloney, F., Wickramaratne, C., et al., 2019. Strategic control and cost optimization of thermal energy storage in buildings using energy plus. Appl. Energy 246, 77–90.
Song, X., Zhu, T., Liu, L., et al., 2018a. Study on optimal ice storage capacity of ice thermal storage system and its influence factors. Energy Convers. Manag. 164, 288–300.
Tam, A., Ziviani, D., Braun, J.E., et al., 2019. Development and evaluation of a generalized rule-based control strategy for residential ice storage systems. Energy Build. 197, 99–111.
Lake, A., Rezaie, B., Beyerlein, S., 2017. Review of district heating and cooling systems for a sustainable future. Renew. Sustain. Energy Rev. 67, 417–425.
Song, X., Liu, L., Zhu, T., et al., 2018b. Study of economic feasibility of a compound cool thermal storage system combining chilled water storage and ice storage. Appl. Therm. Eng. 133, 613–621.
Heine, K., Tabares-Velasco, P.C., Deru, M., 2021. Design and dispatch optimization of packaged ice storage systems within a connected community. Appl. Energy 298, 117147.
Zhao, J., Li, J., Shan, Y., 2021. Research on a forecasted load-and time delay-based model predictive control (MPC) district energy system model. Energy Build. 231, 110631.
Yan, B., Chen, G., Zhang, H., et al., 2021. Strategical district cooling system operation with accurate spatiotemporal consumption modeling. Energy Build., 111165
Cox, S.J., Kim, D., Cho, H., et al., 2019. Real time optimal control of district cooling system with thermal energy storage using neural networks. Appl. Energy 238, 466–480.
D'Ettorre, F., De Rosa, M., Conti, P., et al., 2019. Mapping the energy flexibility potential of single buildings equipped with optimally-controlled heat pump, gas boilers and thermal storage. Sustain. Cities Soc. 50, 101689.
Liu, F., Deng, J., Mo, Q., et al., 2021. Structure and control co-optimization for an ejector expansion heat pump coupled with thermal storages. Energy Build. 235, 110755.
Gelazanskas, L., Gamage, K.A.A., 2014. Demand side management in smart grid: a review and proposals for future direction. Sustain. Cities Soc. 11, 22–30.
Osterman, E., Stritih, U, 2021. Review on compression heat pump systems with thermal energy storage for heating and cooling of buildings. J. Energy Storage 39, 102569.
Baeten, B., Rogiers, F., Helsen, L., 2017. Reduction of heat pump induced peak electricity use and required generation capacity through thermal energy storage and demand response. Appl. Energy 195, 184–195.
Bechtel, S., Rafii-Tabrizi, S., Scholzen, F., et al., 2020. Influence of thermal energy storage and heat pump parametrization for demand-side-management in a nearly-zero-energy-building using model predictive control. Energy Build. 226, 110364.
Dar, U.I., Sartori, I., Georges, L., et al., 2014. Advanced control of heat pumps for improved flexibility of Net-ZEB towards the grid. Energy Build. 69, 74–84.
Schibuola, L., Scarpa, M., Tambani, C., 2015. Demand response management by means of heat pumps controlled via real time pricing. Energy Build. 90, 15–28.
Viot, H., Sempey, A., Mora, L., et al., 2018. Model predictive control of a thermally activated building system to improve energy management of an experimental building: part I—modeling and measurements. Energy Build. 172, 94–103.
Fischer, D., Toral, T.R., Lindberg, K.B., et al., 2014. Investigation of thermal storage operation strategies with heat pumps in German multi family houses. Energy Procedia 58, 137–144.
Meng, Q., Ren, X., Wang, W., et al., 2021. Reduction in on-off operations of an air source heat pump with active thermal storage and demand response: an experimental case study. J. Energy Storage 36, 102401.
Alimohammadisagvand, B., Jokisalo, J., Kilpeläinen, S., et al., 2016. Cost-optimal thermal energy storage system for a residential building with heat pump heating and demand response control. Appl. Energy 174, 275–287.
Arteconi, A., Hewitt, N.J., Polonara, F., 2013. Domestic demand-side management (DSM): role of heat pumps and thermal energy storage (TES) systems. Appl. Therm. Eng. 51, 155–165.
Fitzpatrick, P., D'Ettorre, F., DE Rosa, M., et al., 2020. Influence of electricity prices on energy flexibility of integrated hybrid heat pump and thermal storage systems in a residential building. Energy Build. 223, 110142.
Mazzoni, S., Sze, J.Y., Nastasi, B., et al., 2021. A techno-economic assessment on the adoption of latent heat thermal energy storage systems for district cooling optimal dispatch & operations. Appl. Energy 289, 116646.
Dorotić, H., Pukšec, T., Duić, N., 2019. Multi-objective optimization of district heating and cooling systems for a one-year time horizon. Energy 169, 319–328.
Balboa-Fernández, M., De Simón-Martín, M., González-Martínez, A., et al., 2020. Analysis of district heating and cooling systems in Spain. Energy Rep. 6, 532–537.
Nouidui, T.S., Coignard, J., Gehbauer, C., et al., 2019. CyDER – an FMI-based co-simulation platform for distributed energy resources. J. Build. Perform. Simul. 12, 566–579.
Buffa, S., Cozzini, M., D'antoni, M., et al., 2019. 5th generation district heating and cooling systems: a review of existing cases in Europe. Renew. Sustain. Energy Rev. 104, 504–522.
Sommer, T., Sulzer, M., Wetter, M., et al., 2020. The reservoir network: a new network topology for district heating and cooling. Energy 199, 117418.
Wang, H., 2017. A steady-state empirical model for evaluating energy efficient performance of centrifugal water chillers. Energy Build. 154, 415–429.
Reddy, T.A., Andersen, K.K., 2002. An evaluation of classical steady-state off-line linear parameter estimation methods applied to chiller performance data. HVAC&R Res. (8), 101.
Ashrae Handbook. 2018 HVAC applications. Building operations and management.
Ciulla, G., D'Amico, A., 2019. Building energy performance forecasting: a multiple linear regression approach. Appl. Energy 253, 113500.